

Structure of a Fab Complex with the C-terminal fragment of merozoite surface protein-1 of *Plasmodium vivax* determined by Computational Docking

M.L. Serrano^{a,*}, A. Gauna^b, H.A. Pérez^c, E. Squitieri^b and J.D. Medina^d

^aUnidad de Química Medicinal, Facultad de Farmacia, Universidad Central de Venezuela, Caracas 1041-A, Venezuela

^bEscuela de Química, Facultad de Ciencias, Universidad Central de Venezuela, Apartado 47102, Caracas 1020-A, Venezuela

^cLaboratorio de Inmunoparasitología, Centro de Microbiología y Biología Celular, IVIC, Apartado 21827, Caracas 1020-A, Venezuela

^dUnidad de Productos Naturales, Facultad de Farmacia, Universidad Central de Venezuela, Caracas 1041-A, Venezuela

Abstract. One current vaccine candidate against *Plasmodium vivax*, targeting asexual blood stages, is the major merozoite surface protein-1 of *P. vivax* (PvMSP-1). Vaccine trials with PvMSP-1₁₉ and PvMSP-1₃₃ have succeeded in protecting monkeys and it has been shown that a large proportion of individuals naturally exposed to *P. vivax* infection, develop specific antibodies to PvMSP-1₁₉. In the present study, computational protein-protein docking was used to predict the structure of the antigen-antibody complex between PvMSP1₁₉ and the Fab region of the G17.12 monoclonal antibody. This antibody does not inhibit erythrocyte invasion or MSP1 processing, but it recognises a discontinuous epitope on PfMSP1₁₉ that has been mapped to regions recognised by invasion-inhibiting antibodies. The molecular simulations were performed using, as starting structures, the Fab fragment of the *P. falciparum* MSP1₁₉-mAbG17.12 complex (pdb:1ob1) and the structure of the *P. vivax* MSP1₁₉ previously determined by homology modeling. The mAb was submitted to a docking procedure with antigen PvMSP1₁₉ using the programs PatchDock and FireDock to obtain an initial structure for the complex. A final optimization was performed with RosettaDock using a Monte Carlo algorithm. The final structure of the PvMSP1₁₉-mAb17.12 complex shows that the antibody recognizes a discontinuous epitope that include segments on the first domain and some residues at the end of the second domain. The model provides valuable guidelines for future experimental work devoted to the identification of B-epitopes and synthesis of peptides with antigenic activity.

Keywords: Merozoite surface protein 1, *Plasmodium vivax*, malaria vaccine candidate, antibody – antigen complex, docking

1. Introduction

Malaria today remains as one of the major causes of mortality and morbidity, with 3.2 billion people at risk, 300–500 million clinical cases and more than one million deaths annually [1]. Malaria is

*Corresponding author: María Luisa Serrano; Unidad de Química Medicinal, Facultad de Farmacia, Universidad Central de Venezuela, Caracas, 1041-A, Venezuela. Tel.: +58 212 605 2697; Fax: +58 212 605 2707; E-mail: maria.serrano@ucv.ve.

present in nearly 90 countries with 2.5 billion people exposed to infection by *Plasmodium falciparum* and *Plasmodium vivax* [2]. While *P. falciparum* prevails on the African continent [3], *P. vivax* is the most widespread of the four Plasmodium species; it accounts for more than 50% of all malaria cases outside Africa and is responsible for significant morbidity in South American and Asian regions with a yearly estimate of 80 million cases [4]. During the last two decades, a number of reports have documented the development of resistance in *P. vivax* to several first-line antimalarial drugs [5–7] and the development of new strategies for combating the disease are urgently needed. Furthermore, wide geographic co-endemicity of *P. falciparum* and *P. vivax* results in an additional challenge for diagnosis and treatment.

The major merozoite surface protein-1 (MSP1) of the malaria parasite *P. falciparum* is of considerable interest as a vaccine candidate antigen [8,9]. The C-terminal fragment of MSP1 (PfMSP1₁₉) enclosed two epidermal growth factor (EGF)-like domains and monoclonal antibodies binding MSP1₁₉ have the ability to inhibit the invasion of erythrocytes *in vitro* [10,11] as well as *in vivo* in rodent models [12,13]. It has been suggested that inhibition of MSP1 processing is the mechanism of action of these inhibitory antibodies. However, those antibodies specific for MSP1₁₉ that are not inhibitory can be divided into two classes: blocking antibodies that interfere with the binding of inhibitory antibodies and neutral antibodies which bind to MSP1₁₉ but neither inhibit invasion nor block the binding of inhibitory antibodies [14–16].

Homologue PvMSP1 a 200 kDa protein expressed on the surface of *P. vivax* merozoite, is also a current vaccine candidate against asexual blood stages [17]. Studies on the naturally acquired humoral immune responses against *P. vivax* MSP1, showed that MSP1 C-terminal fragment of *P. vivax* (PvMSP1₁₉) is the most immunogenic portion of the molecule and evidence suggests that immunodominant domains interacting with protective antibodies are related to a structure also containing two epidermal growth factor (EGF)-like domains, like in PfMSP1₁₉ [18,19]. Furthermore, vaccine trials with PvMSP1₁₉ and PvMSP1₃₃ have succeeded in protecting monkeys and it has been shown that a large proportion of individuals naturally exposed to *P. vivax* transmission, develop specific antibodies to PvMSP1₁₉ [20–22].

To date most of the work on MSP1 has been focused on the *Plasmodium falciparum* protein. However, given the serious morbidity of malaria caused by *Plasmodium vivax*, and the wide co-endemicity of these two species, is particularly important for vaccine development to focus on *P. vivax*.

The crystal structures of the C-terminal domains of PcMSP-1 (*P. cynomolgi*) [23], PkMSP-1 (*P. knowlesi*) [24], and the solution structure of PfMSP-1 (*P. falciparum*) [25], have been reported. The *P. vivax* C-terminal fragment of MSP1 has been studied using homology modeling [26] and NMR [27]. Moreover, the binding mode to specific antibodies was subject of different structural studies [28,29]. The crystal structure of PfMSP1₁₉ in complex with the Fab-fragment of mAb G17.12 has been solved [28] and the interaction of PfMSP1₁₉ with malaria parasite inhibitory antibodies was studied by computational docking [29]. The mAb G17.12 does not inhibit erythrocyte invasion or MSP1 processing, but it recognizes a discontinuous epitope comprising 13 residues on the first epidermal growth factor (EGF)-like domain of PfMSP1₁₉ [28]. Because the overall folding of PvMSP1₁₉ is very similar to that previously reported for other C-terminal fragments of MSP-1, comparative studies could provide relevant information for the identification of epitopes helpful for the optimization of vaccines.

X-ray crystallization, while providing complete and high-resolution information, is time consuming and can be limited by the ability of the complex to form a crystal. An alternative is to use computational docking to predict the 3D structure of a protein complex. Our objective is to predict the structure of *P. vivax* MSP1₁₉ in complex with the Fab-fragment of mAb G17.12 by using a protocol that combines the protein docking programs PatchDock [30] and FireDock [31], to obtain the starting structure and RossettaDock [32] to obtain the final model of the complex. In the docking field, protein flexibility

and the absence of robust scoring functions present an important challenge. Due to these difficulties many docking methods apply a two-tier approach: coarse global search for feasible orientations that treats proteins as rigid bodies, followed by an accurate refinement stage that aims to introduce flexibility into the process. The PatchDock web server [30] performed rigid-body docking and then the results were sent to the FireDock web server that provides a method for flexible refinement and scoring the protein–protein docking solutions. The RosettaDock [32] method employs a low-resolution rigid-body Monte-Carlo search followed by an all-atom, simultaneous optimization of backbone displacement and backbone-dependent side chain rotamer conformations by using Monte-Carlo minimization.

In this work we propose a model for the three-dimensional structure of a Fab complex with the C-terminal fragment of merozoite surface protein-1 of *P. vivax* determined by computational docking. The structural data thus obtained reveal the presence of a discontinuous epitope that comprises residues on the first domain of PvMSP₁₉ and in the second domain of the protein.

2. Computational strategy

Modeling studies as well as the generation and analysis of the structures were performed running on AMD Athlon TM 64 X2 Dual Core Processor Driver for Windows XP (3.00 GHz HT). The publicly available web-servers for protein-protein docking PatchDock [30], FireDock [31] and RosettaDock [32] were used for protein docking calculations. The structural alignment and analysis were performed using DeepView/SwissPdb-Viewer 3.7 (Glaxo-SmithKline) [33]. Molecular figures were prepared using WebLab ViewerLite 3.20. The CASTp server was used for identification of the binding sites [34]. CASTp provides identification and analytical measurements of surface accessible pockets, for proteins and other molecules, which can be used to guide protein–protein interactions.

To obtain the starting structures, the crystal structure of the Fab fragment (D and E chains) of the *P. falciparum* MSP1₁₉-FabG17.12 complex (pdb:1ob1) [28] and the structure of the *P. vivax* MSP1₁₉ previously determined by homology modeling [26], were sent to the PatchDock web server. PatchDock is a geometry-based molecular docking algorithm and each candidate solution is evaluated by a scoring function that considers both geometric fit and atomic desolvation energy. The RMSD (root mean square deviation) default clustering was applied to discard redundant solutions [30]. The FireDock web server was used for refinement and re-scoring the 1000 rigid-body protein-protein docking solutions thus obtained. FireDock algorithm includes a Side-chain optimization followed by a Rigid-body minimization by a Monte Carlo technique that attempts to optimize an approximate binding energy and a final ranking stage is performed according to a binding energy function [31]. This protocol was performed 10 times to assess the statistical trends of the solutions. The best average PvMSP1₁₉-FabG17.12 complex model was used as starting structure for a further refinement with RosettaDock. The RosettaDock method employs a low-resolution rigid-body Monte-Carlo search followed by an all-atom, simultaneous optimization of backbone displacement and backbone-dependent side chain rotamer conformations by using Monte-Carlo minimization. The resulting models are ranked by using a scoring function dominated by van der Waals interactions, implicit Gaussian solvation, orientation-dependent hydrogen bonding, side-chain rotamer probabilities and low-weighted electrostatics energy [32,35]. To generate an ensemble of models, the default 1000 independent simulations were carried out. The 10 best-scoring structures from the run ranked by energy were inspected. The final antibody-antigen complex was checked with ProCheck.

The docking of mAb G17.12 with antigen PfMSP1₁₉ was performed as a test case to check the reliability of the docking procedure. The model of the complex thus obtained was compared with the crystal structure previously reported.

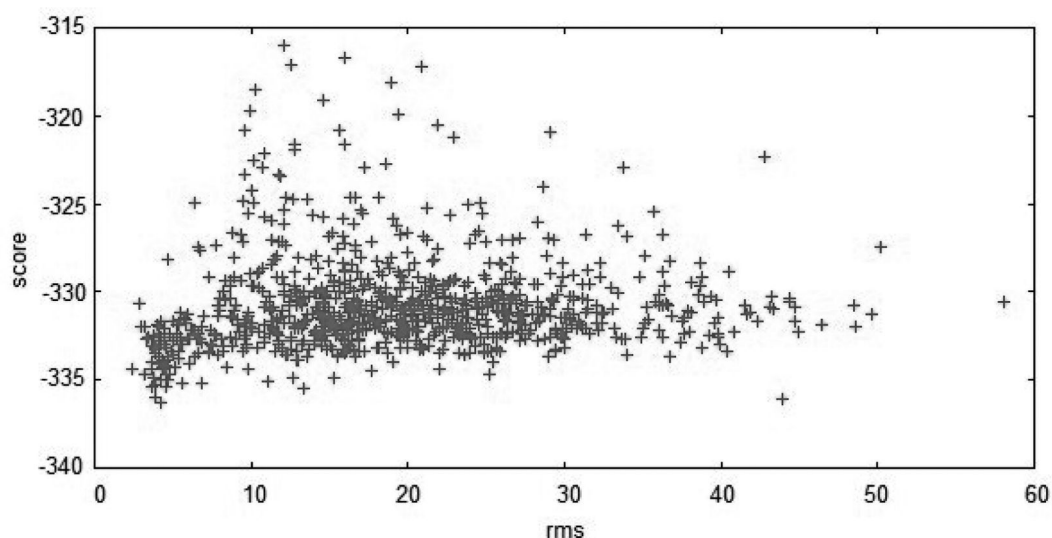


Fig. 1. Perturbation studies on antigen/antibody complex PvMSP1₁₉-FabG17.12. Plot of the energies of the structures created during the docking run versus the RMSD from the starting input conformation.

3. Results and discussion

The prediction of antibody-antigen complex structures is critical to rational vaccine design. Moreover the design process will benefit from understanding the influence of the antigenic protein individual residues on the calculated binding energy. In the present work we performed a molecular docking calculation with the PvMSP1₁₉ and the Fab fragment of the monoclonal antibody G17.12 to investigate which residues are especially important as binding epitopes.

The overall protocol for the determination of the PvMSP1₁₉-mAbG17.12 complex includes, as an initial step, the use in combination of PatchDock and FireDock to obtain the starting structure. We identified the high reproducibility of the protocol when the best solution of each run, as judged by the value of their global energy, was structurally compared and no significant RMSD deviation between them was observed. The model with the lower global energy was saved for further refinement and validation.

Final refinement was performed with RosettaDock, as described in Section 2. The power of RosettaDock method has been repeatedly and successfully tested in CAPRI (**C**ritical **A**ssessment of **P**redicted **I**nteractions) blind tests on diverse targets including antigen-antibody pairs, enzyme-inhibitor pairs and regulatory proteins [36]. As a result of perturbation studies on the PvMSP1₁₉-mAbG17.12 complex, the server returns a plot of the energies of 1000 structures created during the docking run versus the RMSD from the starting input conformation (Fig. 1). The presence of the 'docking funnel', where many low-scoring decoys have similar RMSD values (indicating similar conformations) can be used as convergence criterion and, by extension, to generate confidence in the provided solutions. The lowest energy model obtained by RosettaDock was selected as our prediction for the PvMSP1₁₉-mAbG17.12 complex. The quality of the model was checked with ProCheck. The structure satisfied the tests; in the Ramachandran plot, 96.5% of the non-glycine residues lie within the most favored and additionally allowed regions indicating a good overall geometry of the complex.

Figure 2 shows the relative positions of PvMSP1₁₉ and the mAbG17.12 in the final model and Table 1 shows the residue interface contacts. The interface incorporates 16 residues of the first domain of PvMSP1₁₉, segments 1-9, 12-17, 20, and 6 residues of the second domain, segments 80-84 and 90,

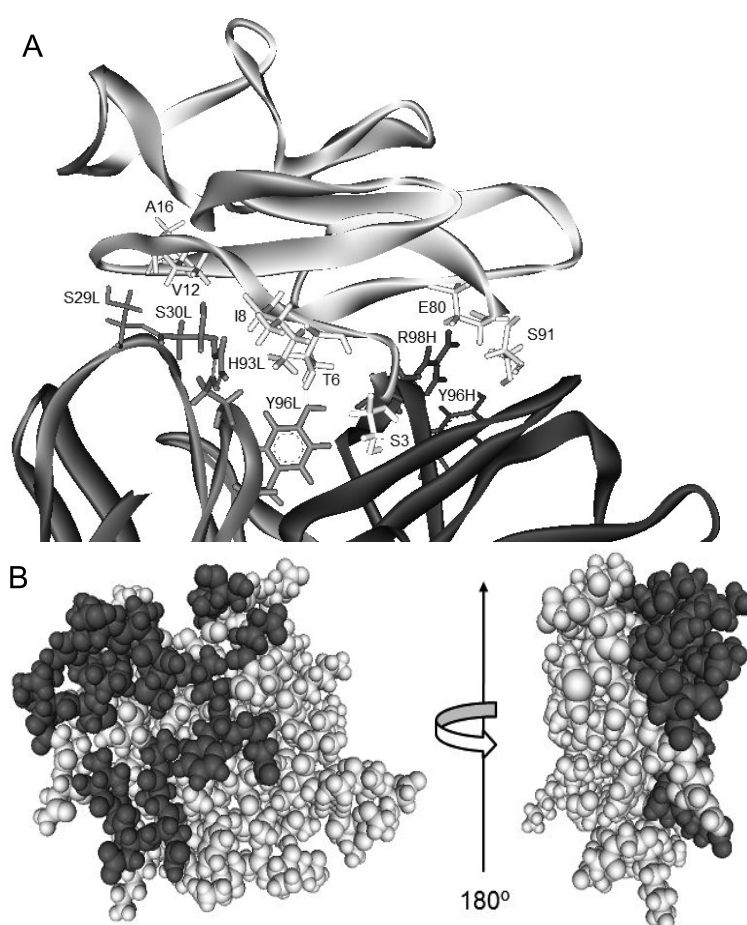


Fig. 2. Panel (A): Ribbon representation of the proposed structure for the PvMSP₁₁₉-mAbG17.12 complex, showing the antigen and the variable domains of the antibody. The VH and VL domains are dark gray and light gray and the *P. vivax* MSP1₁₉ is colored white. Panel (B): Contacting residues for the antigen colored in dark gray.

91. There are seven hydrogen bonds across the interface that accounts for the stability of the complex: I8-H93L, A16-S30L, S91-Y96H, V12-S29L, T6-Y96L, E80-R98H and S3-Y96L (in decreasing order of calculated Rosetta hydrogen bonding energy, where Y96L refers to the Tyr at residue position 96 of the light chain, and so on). Several residue pairs also make extensive hydrophobic contacts: E4-W50H, S3-Y96L, E4-Q58H, S2-Y97H, E80-R98H, S91-T31H, M1-Y97H, I8-H93L, and S3-W50H (in decreasing order of Rosetta van der Waals attractive energies). The intermolecular contacts that contribute the most to the total binding energy in the Rosetta calculations are S3-Y96L, S3-W50H and E80-R98H. As follows from the analysis above, the mAbG17.12 recognizes a discontinuous epitope on the first domain of PvMSP₁₉ and another one in the second domain of the protein.

Previously, when the structure of PvMSP₁₉ was determined by homology modeling [26], the three-dimensional structures of PvMSP₁₉ and PfMSP₁₉ were compared and a less compact structure and a main binding pocket, well suited for protein-protein interactions, were observed for the first domain of the *P. vivax* protein. To add in proof of the previous observation, a careful comparison was performed between our *P. vivax* antigen-antibody model and the results of two different structural studies of *P. falciparum* MSP₁₉ complexes [28,29]. Table 2 shows the residues that are recognized within the

Table 1
Antibody/Antigen interface residues

PvMSP1 ₁₉	mAb G17.12	PvMSP1 ₁₉	mAb G17.12
M1	H: Y97, R98, F99, G100A L: Y32, F91	D14	L: S27A, S29
S2	H: W50, N52, Y97 L: F91	N15	L: S29, S67
S3	H: W47, W50, Q58, N95 L: F91, S94, Y96	A16	L: S29, S30
E4	H: W50, N52, S54, V56, Q58	A17	L: S30, Y32
H5	H: N52, Y97	R20	H: Q58
T6	L: Y32, F91, S94, Y96	E80	H: R98
C7	L: H93	L82	H: Y97, R98
I8	L: H93, S94	F83	H: R98, D100 L: S30, S31, Y32, T50
D9	L: H93	E84	L: N53
V12	L: S29, S30, H92	S90	H: Y97
P13	L: S29	S91	H: T30, A32, Y96, Y97, R98

PvMSP1₁₉ residues that contact the mAbG17.12 in the complex model. The heavy (H) and light (L) chain CDR regions are residues 26–32, 52–55, 92–104 and 26-31, 50-54 and 89–96.

Table 2
Residues of *P. vivax* MSP1₁₉ in contact with mAbG17.12 compared with those of *P. falciparum* MSP1₁₉ in contact with mAb12.10, 12.8 and G17.12

PvMSP1 ₁₉	PfMSP1 ₁₉			PvMSP1 ₁₉	PfMSP1 ₁₉		
	G1712	12.10	12.8		G17.12	12.10	12.8
M1		N 1					D23
S2		I 2					R25
S3							E26
E4		Q4					C28
H5		H5			Y34	Y34	
T6		Q6					G38
C7						D39	D39
I8			V8	V8	K40	K40	
D9			K9	K9		C41	
		Q11	Q11	Q11		E43	
V12		C12		E80			
P13			P13	P13	L82		
D14		Q14	Q14	Q14	F83		
N15		N15	N15		E84	Y84	
A16						F87	
A17				S90			
R20				S91			

PvMSP1₁₉-mAbG17.12 modeled structure and those of the different PfMSP1₁₉-mAb structures.

In the X-ray structure of the PfMSP1₁₉-mAbG17.12 a very similar discontinuous epitope is recognized on the first EGF like domain of the protein [28] (Table 2). This region is particularly interesting because several growth inhibitory monoclonal antibodies (mAb) bind to the first EGF domain of the PfMSP-1₁₉ [37] and, for some of these antibodies, a target epitope has been located on the N-terminal EGF-like domain of the PfMSP1₁₉ [38]. Moreover, mutagenesis studies established that residues R20, E24 and E26 affect the binding of invasion-inhibiting and blocking antibodies [38]. Although the mAbG17.12 is not blocking or inhibitory it recognizes an epitope that includes, among others, some of the residues mentioned above, for both PvMSP1₁₉ and PfMSP1₁₉ complexes.

In the computational docking study about the interaction of PfMSP1₁₉ with two strongly inhibitory antibodies (designated 12.8 and 12.10) two slightly different binding modes were determined for the two antibodies [29]. The PfMSP1₁₉-mAb12.10 complex shows that the antibody recognizes a discontinuous epitope on the first domain and some residues at the end of the second domain [29]. However, for the complex PfMSP1₁₉-mAb12.8 the antigen is anchored mainly through its first EGF-like domain. These observations are in agreement with previous experimental evidences that pointed out that antibody 12.10 can only binds in the presence of both PfMSP1₁₉ EGF domains; while for 12.8 the presence of domain 1 is sufficient to observe binding [37].

From the previous comparison it is clear that our computed structure shows a slightly different binding mode to that observed in the PfMSP1₁₉ complexes. Some of the residues of PvMSP1₁₉ in direct contact with G17.12 correspond to sites that are also recognized in the crystal structure of the PfMSP1₁₉-mAbG17.12 and in the docked complex PfMSP1₁₉-mAb12.8, but it is noteworthy that the *P. vivax* protein is anchored to the antibody through residues that are also recognized in the computed complex of PfMSP1₁₉ with the inhibitory antibody 12.10. Supporting these observations, several studies show the possibility of cross-recognition between-species [39–41].

These results can be considered as an extremely useful, inexpensive and rapid alternative to identify potential B-cell epitopes through the analysis of the computationally determined PvMSP1₁₉-mAbG17.12 complex, especially because no X-ray or NMR studies are available. The model will also provide a working hypothesis for further analysis though it is consistent with previously reported studies that showed that the C-terminal fragment of the PvMSP1 is highly immunogenic and that the immunodominant domains interacting with protective antibodies are related to the EGF domains.

4. Conclusions

The three-dimensional structure of the Fab fragment of the monoclonal antibody G17.12 complex with the C-terminal fragment of merozoite surface protein-1 of *Plasmodium vivax* was determined by computational docking. A successful docking procedure that combines PatchDock, FireDock and RossettaDock, to obtain the final model of the complex, was applied. The PvMSP1₁₉-mAb17.12 complex shows that the antibody recognizes a discontinuous epitope that includes segments on the first domain and some residues at the end of the second domain. There are interesting similarities between our model and the complex of PfMSP1₁₉ with the inhibitory antibody 12.10 previously reported [29].

Acknowledgments

We thank the Instituto de Investigaciones Farmaceuticas and the Consejo de Desarrollo Cientifico y Humanistico of the Universidad Central de Venezuela (UCV) (PG-06-00-6564-2006) and the Instituto Venezolano de Investigaciones Cientificas (IVIC) for financial support.

References

- [1] World Health Organization (2005) World Malaria Report 2005. WHO, Geneva.
- [2] C.A. Guerra, R.W. Snow and S.I. Hay, Mapping the global extent of malaria in 2005, *Trends Parasitol* **22** (2006), 353–358.

- [3] J.G. Breman, The ears of the hippopotamus: manifestations, determinants, and estimates of the malaria burden, *Am J Trop Med Hyg* **64** (2001), 1–11.
- [4] K. Mendis, B.J. Sina, P. Marchesini and R. Carter, The neglected burden of *Plasmodium vivax* malaria, *Am J Trop Med Hyg* **64** (2001), 97–106.
- [5] J.K. Baird, Chloroquine resistance in *Plasmodium vivax*, *Antimicrob Agents Chemother* **48** (2004), 4075–4083.
- [6] S. Pukrittayakamee, K. Chotivanich, A. Chantha, R. Clemens, S. Looareesuwan and N.J. White, Activities of artesunate and primaquine against asexual- and sexual-stage parasites in falciparum malaria, *Antimicrob Agents Chemother* **48** (2004), 1329–1334.
- [7] A.E. Arias and A. Corredor, Low response of Colombian strains of *Plasmodium vivax* to classical antimalarial therapy, *Trop Med Parasitol* **40** (1989), 21–23.
- [8] A.F. Egan, M.J. Blanckman and D.C. Kaslow, Vaccine efficacy of recombinant *Plasmodium falciparum* merozoite surface protein 1 in malaria-naïve, -exposed and/or -re-challenged *Aotus vociferans* monkeys, *Infect Immun* **68** (2000), 1418–1427.
- [9] A.W. Stower, V. Cioce, R.L. Shimp et al., Efficacy of two alternate vaccines based on *Plasmodium falciparum* merozoite surface protein 1 in an *Aotus* challenge trial, *Infect Immun* **69** (2001), 1536–1546.
- [10] M.J. Blackman, H.G. Heidrich, S. Donachie, J.S. McBride and A.A. Holder, A single fragment of a malaria merozoite surface protein remains on the parasite during red cell invasion and is the target of invasion-inhibiting antibodies, *J Exp Med* **172** (1990), 379–382.
- [11] M.J. Blackman, T.J. Scott-Finnigan, S. Shai and A.A. Holder, Antibodies inhibit the protease-mediated processing of a malaria merozoite surface protein, *J Exp Med* **180** (1994), 389–393.
- [12] S. Kumar, A. Yadava, D.B. Keister et al., Immunogenicity and *in vivo* efficacy of recombinant *Plasmodium falciparum* merozoite surface protein-1 in *Aotus* monkeys, *Mol Med* **1** (1995), 325–332.
- [13] S. Kumar, W. Collins, A. Egan et al., Immunogenicity and efficacy in *Aotus* monkeys of four recombinant *Plasmodium falciparum* vaccines in multiple adjuvant formulations based on the 19-kilodalton C terminus of merozoite surface protein 1, *Infect Immun* **68** (2000), 2215–2223.
- [14] J.A. Guevara Patino, A.A. Holder, J.S. McBride and M.J. Blackman, Antibodies that inhibit malaria merozoite surface protein-1 processing and erythrocyte invasion are blocked by naturally acquired human antibodies, *J Exp Med* **186** (1997), 1689–1699.
- [15] R.I. Nwuba, O. Sodeinde, C.I. Anumudu, Y.O. Omosun, A.B. Odaibo, A.A. Holder and M. Nwagwu, The human immune response to *Plasmodium falciparum* includes both antibodies that inhibit merozoite surface protein-1 secondary processing and blocking antibodies, *Infect Immun* **70** (2002), 5328–5331.
- [16] C. Dekker, C. Uthairipibull, L.J. Calder, M. Lock, M. Grainger, W.D. Morgan, G.G. Dodson and A.A. Holder, Inhibitory and neutral antibodies to *Plasmodium falciparum* MSP1₁₉ form ring structures with their antigen, *Mol Biochem Parasitol* **137** (2004), 143–149.
- [17] H.A. del Portillo, S. Longacre, E. Khouri and P.H. David, Primary structure of the merozoite surface antigen 1 of *Plasmodium vivax* reveals sequences conserved between different *Plasmodium* species, *Proc Natl Acad Sci USA* **88** (1991), 4030–4034.
- [18] I.S. Soares, G. Levitus, J.M. Sousa, H.A. Del Portillo and M.M. Rodrigues, Acquired immune responses to the N- and C-terminal regions of *Plasmodium vivax* merozoite surface protein 1 in individuals exposed to malaria, *Infect Immun* **65** (1997), 1606–1614.
- [19] I. Holm, F. Nato, K.N. Mendis and S. Longacre, Characterization of C-terminal merozoite surface protein 1 baculovirus recombinant proteins from *Plasmodium vivax* and *Plasmodium cynomolgi* as recognised by the natural anti-parasite immune response, *Mol Biochem Parasitol* **89** (1997), 313–319.
- [20] W.E. Collins, D.C. Kaslow, J.S. Sullivan, C.L. Morris, G.G. Galland, C. Yang, A.M. Saekhou, L. Xiao and A.A. Lal, Testing the efficacy of a recombinant merozoite surface protein (MSP-119) of *Plasmodium vivax* in *Saimiri boliviensis* monkeys, *Am J Trop Med Hyg* **60** (1999), 350–356.
- [21] C. Yang, W.E. Collins, J.S. Sullivan, D.C. Kaslow, L. Xiao and A.A. Lal, Partial protection against *Plasmodium vivax* blood-stage infection in *Saimiri* monkeys by immunization with a recombinant C-terminus of merozoite surface protein 1 (MSP-1) in block copolymer adjuvant, *Infect Immun* **67** (1999), 342–349.
- [22] A.Y. Sierra, C.A. Barrero, R. Rodriguez, Y. Silva, C. Moncada, M. Vanegas and M.A. Patarroyo, Splenectomised and spleen intact *Aotus* monkeys' immune response to *Plasmodium vivax* MSP-1 protein fragments and their high activity binding peptides, *Vaccine* **21** (2003), 4133–4144.
- [23] V. Chitarra, I. Holm, G.A. Bentley, S. Pe'tres and S. Longacre, The crystal structure of C-terminal merozoite surface protein-1 at 1.8 Å resolution, a highly protective malaria vaccine candidate, *Mol Cell*, **3** (1999), 457–464.
- [24] S.C. Garman, W.N. Simcoke, A.W. Stowers and D.N. Garboczi, Structure of the C-terminal domains of merozoite surface protein-1 from *Plasmodium knowlesi* reveals a novel histidine binding site, *J Biol Chem* **278** (2003), 7264–7269.
- [25] W.D. Morgan, B. Birdsall, T.A. Frenkiel, M.G. Gradwell, P.A. Burghaus, S.E. Syed, C. Uthairipibull, A.A. Holder and J. Feeney, Solution structure of an EGF module pair from the *Plasmodium falciparum* merozoite surface protein 1, *J Mol Biol* **289** (1999), 113–122.

- [26] M.L. Serrano, H.A. Perez and J.D. Medina, Structure of C-terminal fragment of merozoite surface protein-1 from *Plasmodium vivax* determined by homology modeling and molecular dynamics refinement, *Bioorg Med Chem*, **14** (2006), 8359–8365.
- [27] J.J. Babon, W.D. Morgan, G. Kelly, J.F. Eccleston, J. Feeney and A.A. Holder, Structural studies on *Plasmodium vivax* merozoite surface protein-1, *Mol Biochem Parasitol* **153** (2007), 31–40.
- [28] J. C. Pizarro, V. Chitarra, D. Verger, I. Holm, S. Peñares, S. Dartevielle, F. Nato, S. Longacre and G.A. Bentley, Crystal Structure of a Fab Complex Formed with PfMSP1-19, the C-terminal Fragment of Merozoite Surface Protein 1 from *Plasmodium falciparum*: A Malaria Vaccine Candidate, *J Mol Biol*, **328** (2003), 1091–1103.
- [29] F. Autore, S. Melchiorre, J. Kleinjung, W.D. Morgan and F. Fraternali, Interaction of Malaria Parasite-Inhibitory Antibodies with the Merozoite Surface Protein MSP1₁₉ by Computational Docking, *PROTEINS: Structure, Function, and Bioinformatics* **66** (2007), 513–527.
- [30] D. Schneidman-Duhovny, Y. Inbar, R. Nussinov and H.J. Wolfson, PatchDock and SymmDock: servers for rigid and symmetric docking, *Nucl Acid Res* **33** (2005), W363–W367.
- [31] E. Mashiaeh, D. Schneidman-Duhovny, N. Andrusier, R. Nussinov and H.J. Wolfson, FireDock: a web server for fast interaction refinement in molecular docking, *Nucl Acid Res* **36** (Web Server issue) (2008), W229–W232.
- [32] S. Lyskov and J.J. Gray, The RosettaDock server for local protein-protein docking, *Nucl Acid Res* **36** (Web Server Issue) (2008), W233–W238.
- [33] N. Guex and M.C. Peitsch, SWISS-MODEL and the Swiss-PdbViewer: An environment for comparative protein modeling, *Electrophoresis* **18** (1997), 2714–2723.
- [34] T.A. Binkowski, S. Naghibzadeg and J. Liang, CASTp: computed atlas of surface topography of proteins, *Nucleic Acid Res* **31** (2003), 3352–3355.
- [35] J.J. Gray, S.E. Moughan, C. Wang, O. Schueler-Furman, B. Kuhlman, C.A. Rohl and D. Baker, Protein-Protein Docking with Simultaneous Optimization of Rigid-Body Displacement and Side-Chain Conformations, *J Mol Biol* **331** (2003), 281–299.
- [36] J. Janin, K. Henrick, J. Moulton, L.T. Eyck, M.J. Sternberg, S. Vajda, I. Vakser and S.J. Wodak, CAPRI: a critical assessment of predicted interactions, *Proteins*, **52** (2003), 2–9.
- [37] J.A. Chappel and A.A. Holder, Monoclonal antibodies that inhibit *Plasmodium falciparum* invasion *in vitro* recognize the first growth factor-like domain of merozoite surface protein-1, *Mol Biochem Parasitol* **60** (1993), 303–312.
- [38] C. Uthairipillai, B. Aufiero, S.E.H. Syed, B. Hansen, J.A. Guevara Patiño, E. Angov, I.T. Ling, K. Fegeding, W.D. Morgan, C. Ockenhouse, B. Birdsall, J. Feeney, J.A. Lyon and A.A. Holder, Inhibitory and Blocking Monoclonal Antibody Epitopes on Merozoite Surface Protein 1 of the Malaria Parasite *Plasmodium falciparum*, *J Mol Biol* **307** (2001), 1381–1394.
- [39] A. Valderrama-Aguirre, G. Quintero, A. Gómez, A. Castellanos, Y. Pérez, F. Méndez, M. Arévalo-Herrera and S. Herrera, Antigenicity, Immunogenicity, And Protective Efficacy of *Plasmodium Vivax* MSP1 Pv2001: A Potential Malaria Vaccine Subunit, *Am J Trop Med Hyg* **73** (Suppl 5) (2005), 16–24.
- [40] Y. Nagao, M. Kimura-Sato, P. Chavalitsheewinkoon-Petmitr, S. Thongrungrat, P. Wilairatana, T. Ishida, P. Tan-ariya, J.B. de Souza, S. Krudsood and S. Looareesuwan, Suppression of *Plasmodium falciparum* by serum collected from a case of *Plasmodium vivax* infection, *Malaria Journal* **7** (2008), 1–8.
- [41] L. Xu, X. Pei, K. Berzins and A. Chaudhuri, *Plasmodium yoelii*: Experimental evidences for the conserved epitopes between mouse and human malaria parasite, *Plasmodium falciparum*, *Exp Parasitol* **116** (2007.) 214–224.